Inform : Jurnal Ilmiah Bidang Teknologi Informasi dan Komunikasi
Vol.11 No.1, January 2026, P-ISSN : 2502-3470, E-ISSN : 2581-0367

Development of a Type-2 Fuzzy Algorithm for Quadplane Attitude Control System in VTOL to Cruising Transition

Meilaillatul Rohmah[1], Purwadi Agus Darwito[2]

[1, 2]*Industrial Technology and Systems Engineering Department, Institut Teknologi Sepuluh Nopember, Surabaya, Indonesia*

[1]meilaillatulr@gmail.com (*)
[2]padarwito@gmail.com

Received: 2025-01-18; Accepted: 2025-11-26; Published: 2026-01-09

Abstract— The Quadplane uncrewed aerial vehicle (UAV) is a combination of a quadcopter system and a conventional aircraft. The Quadplane UAV has three phases: vertical take-off, transition, and cruise. In the transition phase, the Quadplane Tilt-rotor tilts the two front motor axes for forward propulsion. During this transition phase, the aircraft's balance changes, potentially causing it to crash. This study proposes using a type-2 fuzzy control method. The type-2 fuzzy control method is better at handling uncertainties in the Quadplane, known as the Footprint of Uncertainties (FOU), than the type-1 fuzzy method. In this study, simulations were conducted using MATLAB Simulink, and the results of the type-2 fuzzy control method and the PID method from previous studies were compared. The results of the z-position tracking response using the type-2 fuzzy method yield a rise time of ±3 s, an overshoot of <2%, and a steady-state error of ±0.5 m. The results of the x-position tracking response using the type-2 fuzzy method yield a rise time of ±2.5 s, an overshoot of almost 0%, and a steady-state error of <0.2 m. The results of the Quadplane pitch angle position tracking response using the type-2 fuzzy method produce a rise-time value of ±1.5 s, overshoot ±0.05°, steady state error ±0.02Overall, the type-2 fuzzy controller is proven to be more effective, accurate, and efficient in controlling the hybrid Quadplane in the transition phase, so it is worthy of being implemented in a real prototype with hardware-in-the-loop testing as further research.

Keywords— Uncrewed Aerial Vehicle; Quadplane Attitude; Control System; VTOL; Transition Phase; Fuzzy Type-2; PID Method.

I. INTRODUCTION

A Quadplane UAV is a combination of a quadcopter system and a conventional aircraft [1]. The merger of these two systems is intended to produce an uncrewed aerial vehicle (UAV), commonly known as a Quadplane, capable of vertical take-off and landing (VTOL), also with longer flight endurance. This merger resulted in an aircraft system with a forward thrust mechanism added after take-off [1][2]. The advantage of the VTOL system on a quadcopter is that it can be used in urban areas and confined spaces [1]. In addition, the VTOL system can be used in mountainous areas [3] and on small landing areas, and it does not require runways for take-off and landing [4]. However, quadcopters can only fly for short periods, which limits their ability to carry out missions that require a wide range and long endurance. Quadplane UAVs offer several advantages, including lower operating costs than other models, the ability to operate effectively even in unfavourable and dangerous conditions, and greater flight endurance [5].

Due to the addition of a forward thrust mechanism after take-off, the Hybrid Quadplane undergoes a transition phase in which the aircraft changes from VTOL to hovering to cruising. This transition-phase scenario starts with a vertical take-off using 4 propellers to the desired altitude, then the quadplane is in a hovering position. Then the propeller accelerates to the required airspeed. At this phase, the lift force of the hover engine is substituted by the lift force of the aircraft's wings. The propellers slowly reduce their speed to maintain altitude during this period [6]. When the Quadplane transitions from hover mode to cruising mode, or forward flight, the unstable aerodynamic effects change significantly [7][8]. In this transition phase, the aircraft's balance condition changes over time, requiring an appropriate control method to stabilize it [9].

In addition, this phase is susceptible to external disturbances, such as wind. The impact of wind disturbances on UAVs is becoming increasingly significant [10][11][12] and is gradually becoming a major cause of UAV accidents [13]. Quad-Plane is very sensitive to wind disturbances at ground level, making it challenging to keep the aircraft stable in the air, let alone complete its work. In addition, the aircraft may crash [14].

In previous research, several control methods have been used in quadcopter UAV systems. These include PID control [15], linear quadratic control [15][16], and predictive control [15]. When using these three control methods, they produce good results in running the quadcopter, but only to a certain extent, because most of their system models assume no external or internal uncertainty and treat the system model as correct. However, in actual quadcopter control, there are uncertainties in operation and environmental disturbances.

Meanwhile, fuzzy control is considered an alternative. This method is simple and effectively addresses operational uncertainty in quadcopters [17]. Research [18] found that the fuzzy logic method achieved 88.89% accuracy. The implementation of fuzzy algorithms can yield an output value that serves as a reference for the actuator's logic in maintaining the system condition at the set point [19].

Based on previous research on control methods for VTOL UAVs, this research proposes a fuzzy control method. This method is divided into type-1 and type-2 fuzzy sets. The type-2 fuzzy control method can better handle the uncertainty encountered in the quadcopter, also known as the Footprint of Uncertainties, than type-1 [20]. This control method also

DOI : https://doi.org/10.25139/inform.v11i1.9644

handles higher levels of uncertainty compared to type-1 fuzzy control methods [17].

This research will use a type-2 fuzzy control method to address the uncertainty of the Quadplane UAV during the transition phase. The results of the Euler quadplane angle control response using the type-2 fuzzy control method will be compared with those of the previously implemented PID control method in MATLAB. This research aims to determine the effectiveness of type-2 fuzzy control methods on the stability of the Quadplane during the transition phase.

II. RESEARCH METHODOLOGY

A. *Design and Parameter Quadplane*

This research uses a Quadplane design reference from Pavan N's 2020 research. The Quadplane UAV researched this time uses the concept of a fixed-wing aircraft with tilted rotors for Vertical Take-off and Landing and as an aircraft thruster during cruising: data, statistics, and aircraft standards based on Pixhawk aircraft in Fig. 1 [21].

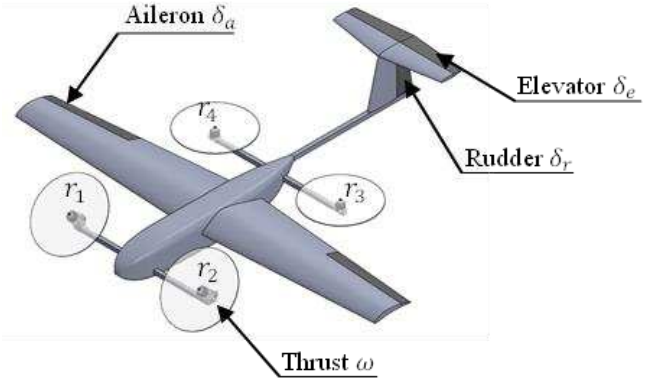

(a) Quadplane Configuration

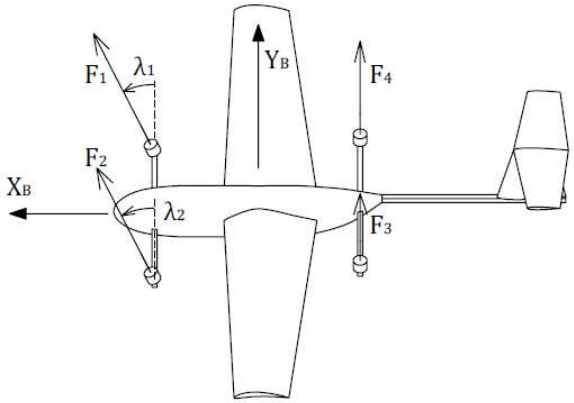

(b) Quadplane Force Direction
Fig.1. Quadplane Design

This study will design a Quadplane control system for the transition phase (hovering to cruising) using a type-2 fuzzy control method. The purpose of designing this control system is to stabilize the Quadplane so it can hover and move forward without falling. To maintain the Quadplane's position so it does not fall, the main thing is to control its pitch angle. This is because the angle affects the Quadplane's direction of movement while cruising.

The parameters required for the transition phase are the z value as the Quadplane hovering coordinate point, the x value as the Quadplane destination coordinate point when cruising, and the pitch angle (θ) of the propeller axis, which needs to be controlled in the transition phase because it affects the direction of the Quadplane's movement when cruising. The y value and yaw angle (ψ) are ignored in this study. Table I for the set point values used in this study.

TABLE I
Parameter X, Y, and Θ Values

Mode	Z Value	X Value	Θ Value
Take-off	0	0	0°
Transition	50	0	90°
Cruising	50	100	90°

This study uses IMU and GPS sensors to detect the Quadplane's position and orientation in 3 dimensions (*X, Y, Z*). These two sensors will produce signals z_a, x_a, θ_a, which are the actual z-position, x-position, and pitch angle of the Quadplane's propeller axis, respectively. The error between the set point and the Quadplane's actual value will generate an input signal for the controller. In this study, the control method used is type-2 fuzzy control. The controller's output signal will serve as the input to servo actuators 1 and 2, as well as motor actuators 1, 2, 3, and 4, to control the speed of these motors during the transition phase. The block diagram of the Quadplane system control during the transition phase is shown in Fig.2

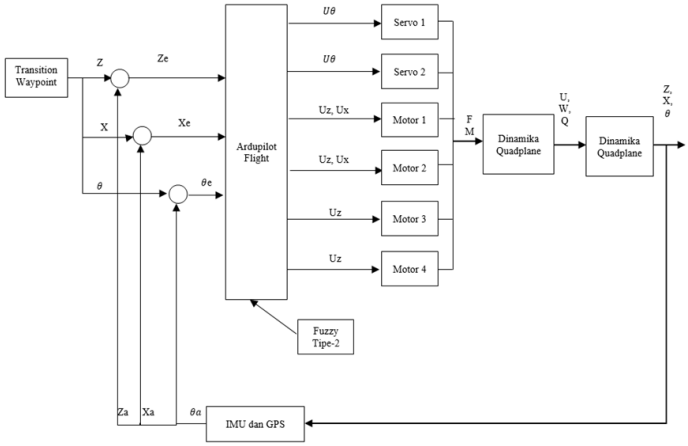

Fig.2. Quadplane Attitude Control Block Diagram During Phase Transition

Fig.2 illustrates the block diagram of the quadplane attitude control system during the transition phase. The sensor block, controller, actuator, and input and output signals in the Quadplane position control system during the transition phase. When the Quadplane reaches the z value corresponding to the setpoint, the Altitude Controller will generate a U_θ control signal. The U_θ will command Servo 1 and Servo 2 to tilt the two front motor axes of the Quadplane, known as the tilt movement. The U_z becomes the control signal input for actuator motors 1, 2, 3, and 4. The U_x becomes the control

DOI : https://doi.org/10.25139/inform.v11i1.9644

signal input for motors 1 and 2. This is because in cruising flight mode, only the two front motors of the Quadplane provide propulsion.

B. Mathematical Model of Quadplane

The mathematical model of a 6 DOF quadplane [22] in all modes can be expressed in Equation (1) [23]. Where, X is represent state variables, U_p is plane control variable, and U_Q is quadcopter control variable. State variables composed of several variables. First, position variables (x, y, z) relative to the inertial frame. Second, linear velocity (u, v, w) relative to the body frame. Third, Euler angles (ϕ, θ, ψ). And fourth, angular velocity (p, q, r) relative to the body frame [24]. The control variables are divided into several variables. First, the rotation speed of the four lift motors in quadcopter mode (m_1, m_2, m_3, m_4), Second, the rotation speed of the pusher motor (pusher) δ_{thr}, elevator deflection (δ_e), aileron deflection (δ_a), and rudder deflection (δ_r).

$$\dot{X} = f(X, U_P, U_Q) \tag{1}$$
$$X = [x \quad y \quad z \quad u \quad v \quad w \quad \phi \quad \theta \quad \psi \quad p \quad q \quad r]^T$$
$$U_p = [\delta_a \quad \delta_e \quad \delta_r \quad \omega]^T, U_Q = [m1 \quad m2 \quad m3 \quad m4]^T$$

To obtain a mathematical model of Quadplane motion, kinematic and dynamic models were developed. This resulted in kinematics defined by coordinate-frame transformations in Equations 2 and 3 [22][23], as follows:

$$\begin{bmatrix} \dot{x} \\ \dot{y} \\ \dot{z} \end{bmatrix} = \begin{bmatrix} \cos\theta\cos\psi & \sin\phi\sin\theta\cos\psi - \cos\phi\sin\psi & \cos\phi\sin\theta\cos\psi + \sin\phi\sin\psi \\ \cos\theta\sin\psi & \sin\phi\sin\theta\sin\psi + \cos\phi\cos\psi & \cos\phi\sin\theta\sin\psi - \sin\phi\cos\psi \\ -\sin\theta & \sin\phi\cos\theta & \cos\phi\cos\theta \end{bmatrix} \begin{bmatrix} u \\ v \\ w \end{bmatrix} \tag{2}$$

$$\begin{bmatrix} \dot{\phi} \\ \dot{\theta} \\ \dot{\psi} \end{bmatrix} = \begin{bmatrix} 1 & \sin\phi\tan\theta & \cos\phi\tan\theta \\ 0 & \cos\phi & -\sin\phi \\ 0 & \sin\phi\sec\theta & \cos\phi\sec\theta \end{bmatrix} \begin{bmatrix} p \\ q \\ r \end{bmatrix} \tag{3}$$

The analysis of quadplane kinetics, mathematical modelling of the quadplane is also obtained from the differential Equations of quadplane dynamics using Equation (4) [23]. Where $\dot{u}, \dot{v}, \dot{w}$ are the first derivative of the linear velocity of quadplane with respect to the quadplane body axis. F_x, F_y, F_z represent the forces on the axis *x, y, z* the quadplane body frame, respectively.

$$\begin{bmatrix} \dot{u} \\ \dot{v} \\ \dot{w} \end{bmatrix} = \begin{bmatrix} rv - qw - g\sin\theta \\ pw - ru + g\sin\phi\cos\theta \\ qu - pv + g\cos\phi\cos\theta \end{bmatrix} + \frac{1}{m}\begin{bmatrix} F_x \\ F_y \\ F_z \end{bmatrix} \tag{4}$$

For the quadplane's rotational motion dynamics, Equation (5) relates to moment balance [23]. Symbol *I* is defined as the matrix of moments of inertia. The symbols M_{roll}, M_{pitch}, and M_{yaw} are the moments of inertia with respect to the x, y, and z axes relative to the quadplane body frame, respectively. The quadplane kinematics and dynamics Equations (6) and (7) will produce a state output using Equation (6), and the integrated state input will be generated using Equation (7) for the desired Quadplane control system.

$$\begin{bmatrix} \dot{p} \\ \dot{q} \\ \dot{r} \end{bmatrix} = I^{-1}\left(-\begin{bmatrix} p \\ q \\ r \end{bmatrix} \times \left(I \begin{bmatrix} p \\ q \\ r \end{bmatrix} \right) + \begin{bmatrix} M_{roll} \\ M_{pitch} \\ M_{yaw} \end{bmatrix} \right) \tag{5}$$

$$\dot{x} = [\dot{X} \quad \dot{Y} \quad \dot{Z} \quad \dot{U} \quad \dot{V} \quad \dot{W} \quad \dot{\phi} \quad \dot{\theta} \quad \dot{\psi} \quad \dot{P} \quad \dot{Q} \quad \dot{R}]^T \tag{6}$$

$$x = [X \quad Y \quad Z \quad U \quad V \quad W \quad \phi \quad \theta \quad \psi \quad P \quad Q \quad R]^T \tag{7}$$

C. Propulsion System

The propulsion motors used in this simulation consist of 4 Emax MT3515 650kv motors with 12x3.8 SF APC propellers. For simplicity, it is assumed that the geometry of the aircraft itself does not interfere with the operation of the propellers. When developing the model, the propeller performance was assumed to depend only on the magnitude and direction of the incoming airflow. Also, the propeller data for the APC 12x3.8 SF propeller was taken from the manufacturer's website [26]. The raw data was used to find the advance ratio (J), thrust coefficient (C_r), torque coefficient (C_q), power coefficient (C_P), and efficiency (η). The definitions of these coefficients are given in Equations (8) to (12).

$$J = \frac{V}{n\,D} \tag{8}$$

$$C_r = \frac{T}{\rho\, n^2\, D^4} \tag{9}$$

$$C_Q = \frac{Q}{\rho\, n^2\, D^5} \tag{10}$$

$$C_P = \frac{P}{\rho\, n^3\, D^5} \tag{11}$$

$$\eta = \frac{C_r\, J}{C_P} \tag{12}$$

The dynamics of the quadplane in fixed-wings mode (after transition) remain closely related to those in VTOL mode. In a broader sense, the aircraft's 6DoF can be separated into two. The first involves the longitudinal axis, and the second involves the lateral and directional axes. Based on the quadplane configuration in Fig.1(a), there are four control variables for aircraft control during fixed-wing mode: Aileron, Elevator, Rudder, and Throttle [21]. The elevator deflection and thrust motor affect the aircraft's longitudinal control. The aileron and rudder affect control in the lateral direction axis. The following are the Equations to determine the deflection of the aileron, elevator, and rudder using Equations (13) to (15), respectively, to produce roll, pitch, and yaw angle values.

$$\delta_a = \delta_{a,trim} + \delta_\phi \tag{13}$$

$$\delta_e = \delta_{e,trim} + \delta_\theta \tag{14}$$

DOI : https://doi.org/10.25139/inform.v11i1.9644

$$\delta_r = \delta_{r,trim} + \delta_\psi \quad (15)$$

D. Propulsion System Forces and Moments

Based on the actuator configuration in Fig.1 (a) and (b), there is a force on the motor axis that must be converted into force and moment relative to the centre of gravity of the aircraft [21]. The aircraft's motors are at right angles to its centre of gravity. The distance between the motors along the x- and y-axes is 0.75 m. The motor positions are given in Equations (16) to (19). The thrust force vectors are given in Equations (20) to (23). The total force generated by the propulsion system is given by Equation (24).

$$r_1 = [0.372 \quad 0.375 \quad 0]^T \quad (16)$$

$$r_2 = [0.372 \quad -0.375 \quad 0]^T \quad (17)$$

$$r_3 = [-0.372 \quad -0.375 \quad 0]^T \quad (18)$$

$$r_4 = [-0.372 \quad 0.375 \quad 0]^T \quad (19)$$

$$F_1 = F_1\,[\sin\lambda_1 \quad 0 \quad -\cos\lambda_1]^T \quad (20)$$

$$F_2 = F_2\,[\sin\lambda_2 \quad 0 \quad \cos\lambda_2]^T \quad (21)$$

$$F_3 = F_3\,[0 \quad 0 \quad -1]^T \quad (22)$$

$$F_4 = F_4\,[0 \quad 0 \quad -1]^T \quad (23)$$

$$F_p = F_1 + F_2 + F_3 + F_4 \quad (24)$$

The moment generated due to propulsion is a combination of the torque generated by the propeller and the moment generated by the thrust force acting at a distance from the CG of the aircraft. The moment acting on the aircraft due to each propeller is given as Equations (25) to (28).

$$Q_1 = Q_1\,[\sin\lambda_1 \quad 0 \quad -\cos\lambda_1]^T \quad (25)$$

$$Q_2 = Q_2\,[\sin\lambda_2 \quad 0 \quad \cos\lambda_2]^T \quad (26)$$

$$Q_3 = Q_3\,[0 \quad 0 \quad -1]^T \quad (27)$$

$$Q_4 = Q_4\,[0 \quad 0 \quad -1]^T \quad (28)$$

The moments acting on the aircraft due to the thrust force of each propeller are given in Equations (29) to (32).

$$M_1 = r_1 \times F_1 \quad (29)$$

$$M_2 = r_2 \times F_2 \quad (30)$$

$$M_3 = r_3 \times F_3 \quad (31)$$

$$M_4 = r_4 \times F_4 \quad (32)$$

The total moment acting on the aircraft due to propulsion is then calculated using Equation (33).

$$M_p = Q_1 + Q_2 + Q_3 + Q_4 + M_1 + M_2 + M_3 + M_4 \quad (33)$$

E. Transition Phase Simulation

The transition phase is when the Quadplane dynamics change from quadcopter to aeroplane dynamics. In this phase, the Quadplane must execute the Quad-to-Plane transition at an airspeed of $0 \le V_a \le 13\,m/s$. In the Quad-to-Plane transition phase, the airspeed is higher than the trim speed ($V_a^c = V_a^* + 2\,m/s$) controlled by the quad-mode controller, and the pusher motor will ramp up until the Quadplane position stabilizes. In this condition, the quad motor is prevented from dropping to zero to prevent an unstable quadplane. Once the airspeed reaches the threshold of $11.2\,m/s$. The aircraft switches to plane-mode control and monitors the trim condition, while quad-mode control drops to zero [23].

In this research, a Quadplane control simulation is conducted in MATLAB Simulink. In this simulation, parameters are specified, including the wind model used and the x, y, and z values. This simulation uses two wind models. The first is the 1-cos discrete wind model. The second is the Von Kármán continuous wind model. The continuous-discrete wind model is defined by Equation (34) [14]. Where t_0 is defined as the time when the wind starts to blow. $V_{W\,max}$ is defined as the highest wind speed. Δt is the interval of time when the wind speed changes.

$$V_W(t_0, \Delta t) = \begin{cases} 0 & t < t_0, \\ \frac{V_{W\,max}}{2}\left(1 - \cos\frac{\pi(t-t_0)}{\Delta t}\right) & t_0 < t < t_0 + \Delta t, \\ V_{W\,max} & t_0 + \Delta t < t, \end{cases} \quad (34)$$

This study uses the Von Kármán continuous wind model to simulate unstable winds. The temporal variations in wind speed are divided into two components, as described by Equation (35). Where $\overline{V_W}$ is the average wind speed over a time period and is defined in Equation (36). T is defined as the duration of the gust. ΔV_W is the fluctuating wind condition. The average time value of ΔV_W is zero. ΔV_W is also used to represent the magnitude of the fluctuation in Equation (37).

$$V_W = \overline{V_W} + \Delta V_W, \quad (35)$$

$$\overline{V_W} = \frac{1}{T}\int_0^T V_W(t)dt, \quad (36)$$

$$\sigma_W^2 = \lim_{T\to\infty}\frac{1}{2T}\int_{-T}^{T}(\Delta V_W(t))^2 dt, \quad (37)$$

Equation (38) defines a spectrum function of the Von Karman wind model. Symbols L_u, L_v, and L_w are defined as the length scales of turbulence in three directions. The symbols $\sigma_{u,W}$; $\sigma_{v,W}$; $\sigma_{w,W}$ are intensity fluctuation functions and altitude-dependent functions.

$$\Phi_{uu}(\Omega) = {\sigma_{u,W}}^2 \frac{L_u}{\pi}\frac{1}{[1+(1.339L_u\Omega)^2]^{5/6}},$$

DOI : https://doi.org/10.25139/inform.v11i1.9644

$$\Phi_{vv}(\Omega) = {\sigma_{v,W}}^2 \frac{L_v}{\pi} \frac{1+8/3(1.339\times 2L_v\Omega)^2}{[1+(1.339L_v\Omega)^2]^{11/6}}, \quad (38)$$
$$\Phi_{ww}(\Omega) = {\sigma_{w,W}}^2 \frac{L_w}{\pi} \frac{1+8/3(1.339\times 2L_e\Omega)^2}{[1+(1.339L_w\Omega)^2]^{11/6}},$$

Equation (39) is defined as the fluctuation intensity and turbulence length scale when the altitude is below 1000 feet. H with (m/s) as the unit is defined as the flying altitude. *u_6* is defined as the wind speed at an altitude of 6 meters.

$$L_w = h,$$
$$L_u = L_v = \frac{h}{(0.177+0.000823h)^{1.2}}, \quad (39)$$
$$\sigma_{w,W} = 0.1u_6,$$
$$\sigma_{u,W} = \sigma_{v,W} = \sigma_{w,W} \frac{1}{(0.177+0.000823h)^{0.4}}$$

F. Fuzzy Logic Controller

Fuzzy logic is a logic with membership degrees in the range 0 to 1, unlike classical Boolean logic [27]. Variables in fuzzy logic are represented in the form of fuzzy sets. Commonly used fuzzy sets are Gaussian, trapezoidal, Gaussian bell, triangular, and sigmoid. In fuzzy logic, the Membership Function (MF) indicates the degree of membership for each value in a variable. The function of the designed fuzzy set is required to determine the degree of membership of fuzzy sets [27]. Fig.3 is an FLC diagram that explains the stages of fuzzy logic control [28].

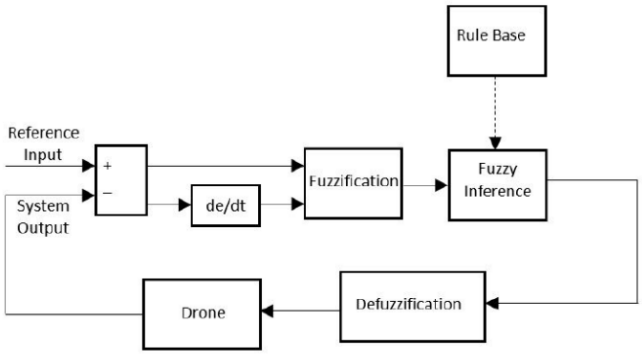

Fig. 3 Fuzzy Logic Control Diagram

A Fuzzy Logic Controller, commonly abbreviated FLC, is a control system that uses the concepts of fuzzy set theory in its design. There are three steps in an FLC, namely fuzzification, inference mechanism, and defuzzification. Fuzzification is the initial step that converts crisp values into fuzzy values. These fuzzy values are then used as input for the inference mechanism. At this step, decisions are made based on the available inputs using a designed logical rule base. Lastly, the fuzzy inference mechanism's output is defuzzified to crisp values [27]. In FLC, a rule base connects input and output values during the fuzzy inference stage. The rules used in this FLC are in the form of "If-Then" [28].

G. Type-2 Fuzzy Logic Controller

Type-2 fuzzy logic can better handle systems with uncertainty and imprecision. This type-2 fuzzy set is essentially a "fuzzy fuzzy." This means that the membership degree of a type-2 fuzzy set is a type-1 fuzzy set. This type-2 fuzzy set was first presented by Zadeh in 1975 [26][27][28]. The classification of type-2 fuzzy sets allows for superior and inferior membership functions; both of these functions can be represented by the respective membership functions of type-1 fuzzy sets. This new concept was introduced by Mendel and Liang in their research [31]. The interval between these two functions is used to describe type-2 fuzzy sets and represents the uncertainty trace (FOU) [30].

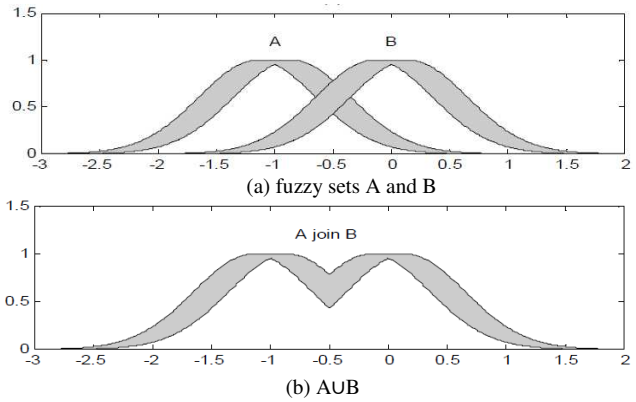

(a) fuzzy sets A and B

(b) AUB

Fig. 4 Type-2 Fuzzy Membership Function

Type-2 fuzzy control systems are commonly defined as an extension of type-1 fuzzy control systems [27]. Type-2 fuzzy logic has two membership functions: primary and secondary. The degree of secondary membership in a type-2 fuzzy logic is 1. The Type-2 fuzzy membership degree is depicted as a uniform shading, as shown in Fig. 4, called the footprint of uncertainty (FOU) [31].

This system also uses an "If-Then" fuzzy rule base. The difference in type-2 fuzzy logic and type-1 fuzzy logic lies in the reduction step after the inference step. Reduction steps convert the output of a type-2 fuzzy set into a type-1 fuzzy set, yielding crisp output values.

III. RESULT AND DISCUSSION

A. Design of Quadplane Transition Phase

This study will design a quadplane control system for the transition phase (from hovering to cruising) using a type-2 fuzzy controller. The control system design aims to stabilize the quadplane's hover and forward motion. The control system design focuses on controlling the *Z, X,* and pitch angles of the quadplane. To implement the transition phase, the simulation requires the *x* and *z* coordinate point parameters as reference points for the hovering/transition phase, along with the angle of the front propeller axis. The x- and z-coordinate values and the propeller axis angle have been determined and are presented in Table I. The parameters controlled by this system include the quadplane's *Z* and *X* positions and pitch angle. And the control parameters used in this study are: 4 propellers as the drive during take-off; 2 front propellers tilted forward and 2 rear propellers slowly slowing to perform the transition phase; 2 front propellers moving constantly; and 2 rear propellers remaining stationary during the cruising phase.

DOI : https://doi.org/10.25139/inform.v11i1.9644

B. *Type-2 Fuzzy Logic Controller Data Representation*

1) Fuzzification: At this stage, crisp inputs will be converted into fuzzy sets. For each FLC parameter input, all three use the Gaussian membership function to achieve fuzzification. Each parameter has one input. The input is the difference between the reference position value and the actual position value for each parameter. The three membership functions for each parameter, namely: x-position, z-position, and tilt angle, are shown in Fig.5.

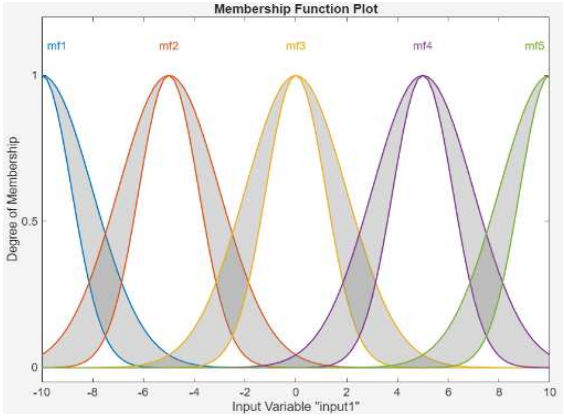

(a) *X* Position

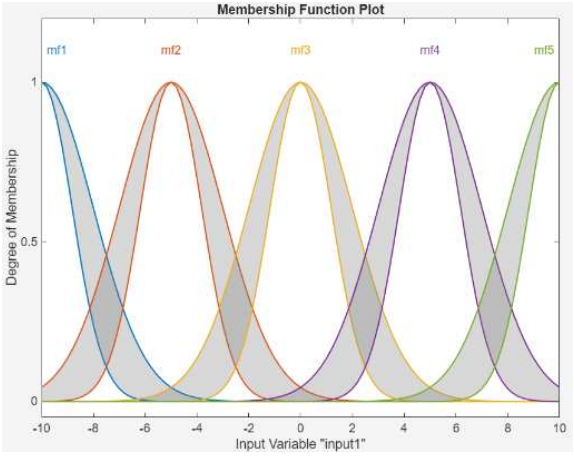

(b) *Z* Position

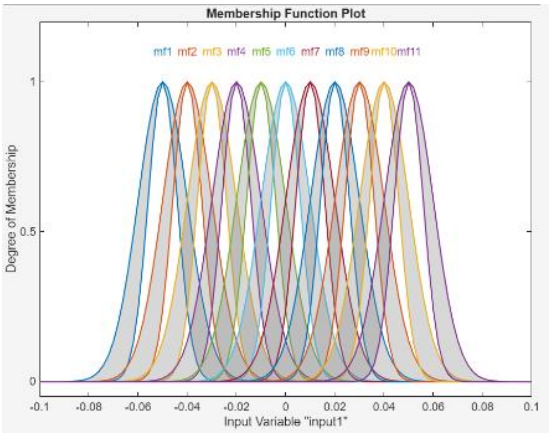

(c) Pitch Angle Position

Fig.5. Membership Function

2) Inference and Rule-Based: Fuzzy rules in the form of "If-Then" are used to connect inputs with outputs at the fuzzy inference stage. In this study, the rule base used to generate the control signal is shown in Fig.6.

	Rule	Weight	Name
1	If input1 is mf1 then output1 is mf1	1	rule1
2	If input1 is mf2 then output1 is mf2	1	rule2
3	If input1 is mf3 then output1 is mf3	1	rule3
4	If input1 is mf4 then output1 is mf4	1	rule4
5	If input1 is mf5 then output1 is mf5	1	rule5

(a) *X* Position

	Rule	Weight	Name
1	If input1 is mf1 then output1 is mf1	1	rule1
2	If input1 is mf2 then output1 is mf2	1	rule2
3	If input1 is mf3 then output1 is mf3	1	rule3
4	If input1 is mf4 then output1 is mf4	1	rule4
5	If input1 is mf5 then output1 is mf5	1	rule5

(b) *Z* Position

	Rule	Weight	Name
1	If input1 is mf1 then output1 is mf1	1	rule1
2	If input1 is mf2 then output1 is mf1	1	rule2
3	If input1 is mf3 then output1 is mf1	1	rule3
4	If input1 is mf4 then output1 is mf1	1	rule4
5	If input1 is mf5 then output1 is mf1	1	rule5
6	If input1 is mf6 then output1 is mf1	1	rule6
7	If input1 is mf7 then output1 is mf1	1	rule7
8	If input1 is mf8 then output1 is mf1	1	rule8
9	If input1 is mf9 then output1 is mf1	1	rule9
10	If input1 is mf10 then output1 is mf1	1	rule10
11	If input1 is mf11 then output1 is mf1	1	rule11

(c) Pitch Angle Position

Fig.6. Rule-Based

3) Type Reduction and Defuzzification: In type-2 fuzzy logic, there is an additional Type-Reduction step that converts the output from a type-2 fuzzy set to a type-1 fuzzy set. This step is necessary to produce a definite output signal. This study also refers to previous research that used the Karnik-Mendel Algorithm for type reduction.

C. *Fuzzy Type-2 Simulation Results*

After determining the data and performing simulations in MATLAB, this section presents the results. Fig.7 shows the results obtained using the type-2 fuzzy method. Fig.7(a) shows that the controller's output can move the Quadplane to the set point at an altitude of 50. However, the altitude value obtained is negative. This is because the flight coordinate system (especially in aircraft and drone simulations) uses the NED (North-East-Down) convention, where the *Z-axis* points downward. To reach the altitude set point, the Quadplane takes 11 seconds. There is no overshoot or drastic change in altitude. Thus, this test shows that the type-2 fuzzy logic can execute the transition phase well, and the Quadplane does not experience a stall (fall). However, there is an error of 0.5 meters. Therefore, the steady-state error value during take-off is 1%.

Fig.7(b) shows the Quadplane's response during cruising along the *x-axis*. The blue line represents x_reff, which is the

DOI : https://doi.org/10.25139/inform.v11i1.9644

set point. The *x*-axis set point is 0 m when the Quadplane takes off and 100 m when it is hovering. A red signal indicating the Quadplane's actual *x* position. During cruising, the Quadplane's actual x position differs from the set point, resulting in an error or a time difference. This causes the Quadplane's rise time to be about 2 seconds slower than the set point value. However, in reaching the *x* coordinate point: 10.

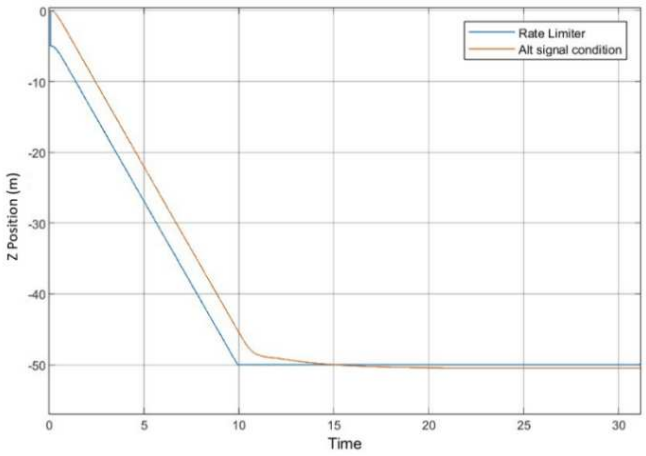

(a) *Z* Position

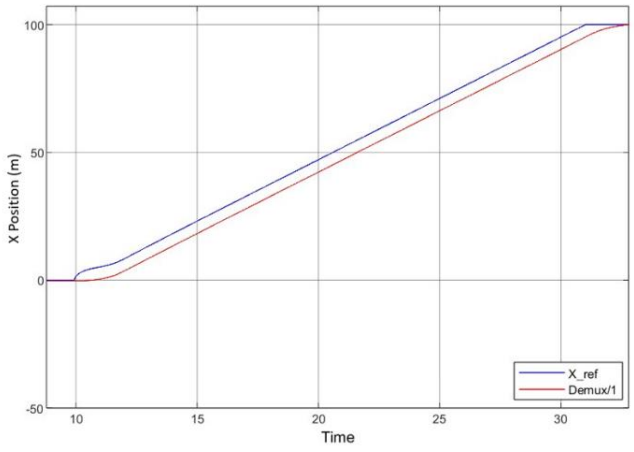

(b) *X* Position

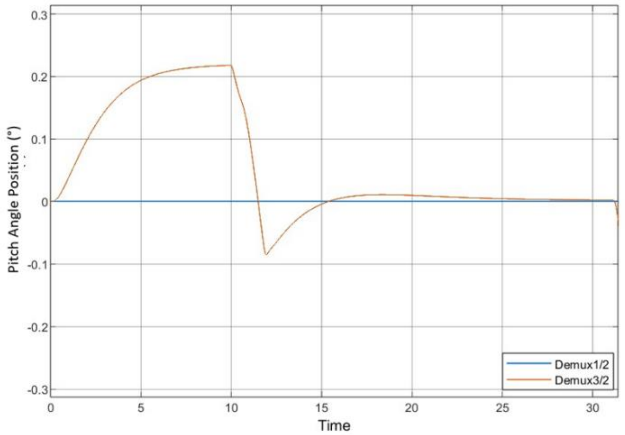

(c) Pitch Angle Position

Fig.7. Simulation Results

Fig.7(c) shows the pitch angle of the Quadplane during take-off until it reaches an altitude of 50 meters, hovering, and cruising for 100 meters. During take-off, the pitch angle changes from 0° to 0.22°. When hovering, the Quadplane's pitch angle changes drastically from 0.2° to -0.09°. During cruising, the pitch angle of the Quadplane reaches a steady state in accordance with the set point and does not experience oscillation.

D. PID Simulation Results

This section presents the results for the PID method. Fig.8 shows the simulation results for the *Z*-position Quadplane, *X*-position Quadplane, and pitch-angle position Quadplane using the PID method. Based on previous simulations, the same response was obtained using type-2 fuzzy logic. First, Fig.8(a) shows that the controller's output can move the Quadplane to the set point at an altitude of 50. The time needed for the Quadplane to reach the set point is 11 seconds. There is no overshoot or drastic change in altitude. Therefore, this test shows that type-2 fuzzy logic performs well during the transition phase, and the Quadplane does not experience a stall (fall).

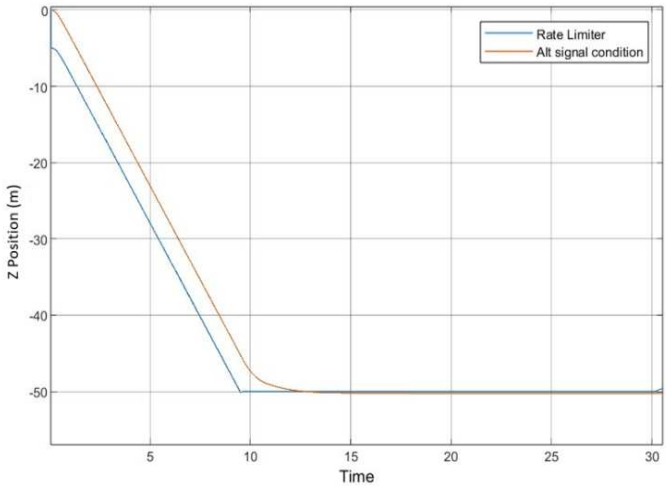

(a) *Z* Position

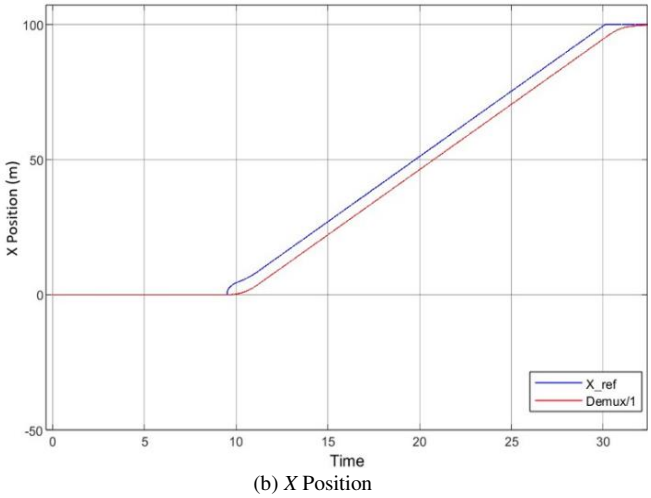

(b) *X* Position

DOI : https://doi.org/10.25139/inform.v11i1.9644

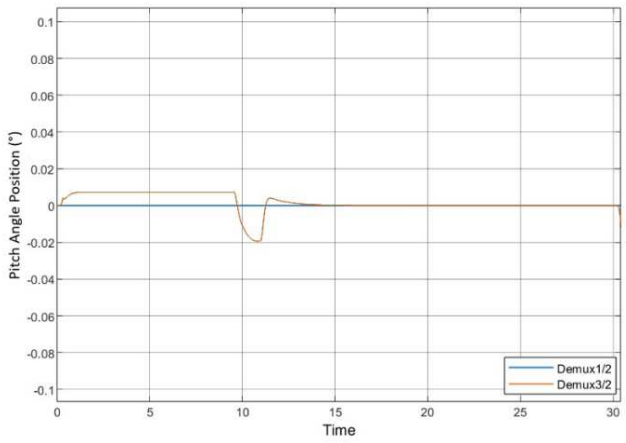

(c) Pitch Angle Position

Fig.8. PID Simulation Result

Fig.8(b) shows that the set point of the x-axis when the Quadplane takes off is 0 m, whereas when the Quadplane is hovering, the set point is 100 m. A red signal indicating the Quadplane's actual x-position. During cruising, the Quadplane's actual x-position differs from the set point, resulting in an error or a time difference. This causes the Quadplane's rise time to be 2 seconds slower than the set point value. However, at the x-coordinate 10, there is no overshoot.

Fig.8(c) shows the results of testing the Quadplane pitch angle position using the PID method. The results of this test show that the red signal corresponds to the Quadplane pitch angle's actual position, and the blue signal corresponds to the Quadplane pitch angle's set point. A change in the Quadplane angle position during take-off. The angle change reached 0.01°. Meanwhile, when the Quadplane is in a hovering condition, the pitch angle changes from 0.01° to 0.02°. This may be due to a change in the direction of the propeller movement, which was initially vertical and then tilted by the servo motor to become horizontal. However, at 12 seconds, the Quadplane's pitch angle returns to 0°, and it then cruises and follows the track properly.

E. Comparison of PID and Fuzzy Type-2 Responses

Fig. 7 and Fig. 8 show the simulation results for the Type-2 Fuzzy Control and PID control methods. Table II below compares the control responses generated by the two control methods.

TABLE II
COMPARISON OF SIMULATION RESULTS USING FUZZY TYPE-2 METHOD AND PID CONTROL METHOD

Parameter	Metric	Fuzzy Type-2	PID	Comparison
X Position	Rise Time	±3 s	±5 s	Fuzzy is faster
	Overshoot	< 2%	±10%	PID has a greater overshoot
	Error steady state	±0,5 m	2–3m	Fuzzy is more accurate
Z Position	Rise Time	±2,5 s	±4 s	Fuzzy is faster
	Overshoot	Almost 0%	±8%	Fuzzy is more stable
	Error steady state	< 0,2m	±1m	Fuzzy is more precise
Pitch Angle Position	Rise Time	±1,5 s	±3 s	Fuzzy is faster
	Overshoot	±0,05°	±0,3°	PID oscillates more
	Error steady state	±0,02°	±0,1°	Fuzzy is more accurate

Based on simulation results, the *z*, *x*, and pitch angle positions of the Quadplane using the two control methods above, namely the type-2 fuzzy method and PID, are shown in Table II. The control system parameters observed and written in the table include: the rise time value of the system in reaching the setpoint, the overshoot that occurs in the system, and the magnitude of the error after reaching the setpoint (steady state error). Table II shows the control response for tracking the Quadplane's x, z positions, and tilt angle. The type-2 fuzzy method yields better results than the PID method. The rise time of the type-2 fuzzy method is faster than that of the PID method in reaching the set point. The overshoot value in the type-2 fuzzy method is relatively smaller than that of the PID method. The steady-state error in the type-2 fuzzy method is smaller than that in the PID method. In addition, in motor and servo control, the type-2 fuzzy method achieves faster rise times than the PID method. The overshoot and steady-state error values using type-2 fuzzy are smaller than those using PID.

IV. CONCLUSION

The designed type-2 fuzzy algorithm successfully controlled the Quadplane hybrid system during the transition phase (hovering to cruising). The controller generated the appropriate thrust distribution across the four motors and adjusted the servo tilt angle responsively, allowing the quadplane to smoothly transition from hovering to cruising without excessive oscillation. Compared to PID control, type-2 fuzzy control shows superior performance with smaller steady-state error, faster settling time, and lower overshoot. The system controlled by the type-2 fuzzy method maintains the balance of X position, Z position, and pitch angle more precisely and efficiently.

The simulation results show that the type-2 fuzzy method effectively validates the Quadplane hybrid system design. This controller provides more accurate tracking, a more stable response, and smoother control signals than PID. This proves that type-2 fuzzy control is an effective method for controlling the Quadplane during the transition phase.

REFERENCES

[1] Y. Govdeli, S. Moheed Bin Muzaffar, R. Raj, B. Elhadidi, and E. Kayacan, "Unsteady aerodynamic modeling and control of pusher and tilt-rotor quadplane configurations," *Aerosp. Sci. Technol.*, vol. 94, Nov. 2019, doi: 10.1016/j.ast.2019.105421.

[2] A. S. Saeed, A. B. Younes, C. Cai, and G. Cai, "A survey of hybrid Unmanned Aerial Vehicles," *Prog. Aerosp. Sci.*, vol. 98, pp. 91–105, Apr. 2018, doi: 10.1016/j.paerosci.2018.03.007.

[3] Ö. Dündar, M. Bilici, and T. Ünler, "Design and performance analyses of a fixed wing battery VTOL UAV," *Eng. Sci. Technol. an Int. J.*, vol. 23, no. 5, pp. 1182–1193, Oct. 2020, doi: 10.1016/j.jestch.2020.02.002.

[4] Y. Li and M. Liu, "Path Planning of Electric VTOL UAV Considering Minimum Energy Consumption in Urban Areas," *Sustainability*, vol. 14, no. 20, p. 13421, Oct. 2022, doi: 10.3390/su142013421.

[5] P. Panagiotou and K. Yakinthos, "Aerodynamic efficiency and

DOI : https://doi.org/10.25139/inform.v11i1.9644

performance enhancement of fixed-wing UAVs," *Aerosp. Sci. Technol.*, vol. 99, p. 105575, 2020, doi: 10.1016/j.ast.2019.105575.

[6] K. Pobikrowska and T. Goetzendorf-Grabowski, "Wind tunnel tests of hovering propellers in the transition state of Quad-Plane," *Bull. Polish Acad. Sci. Tech. Sci.*, vol. 69, no. 6, pp. 1–13, 2021, doi: 10.24425/bpasts.2021.138821.

[7] F. Zhang, X. Lyu, Y. Wang, H. Gu, and Z. Li, "Modeling and Flight Control Simulation of a Quadrotor Tailsitter VTOL UAV," in *AIAA Modeling and Simulation Technologies Conference*, Reston, Virginia: American Institute of Aeronautics and Astronautics, Jan. 2017. doi: 10.2514/6.2017-1561.

[8] B. Mi, H. Zhan, and S. Lu, "An extended unsteady aerodynamic model at high angles of attack," *Aerosp. Sci. Technol.*, vol. 77, pp. 788–801, Jun. 2018, doi: 10.1016/j.ast.2018.03.035.

[9] H. Gu, X. Lyu, Z. Li, S. Shen, and F. Zhang, *Development and Experimental Verification of a Hybrid Vertical Take-Off and Landing (VTOL) Unmanned Aerial Vehicle(UAV)*. 2017. doi: 10.0/Linux-x86_64.

[10] X. Li, B. Zhao, Y. Yao, H. Wu, and Y. Liu, "Stability and Performance Analysis of Six-Rotor Unmanned Aerial Vehicles in Wind Disturbance," *J. Comput. Nonlinear Dyn.*, vol. 13, no. 3, Mar. 2018, doi: 10.1115/1.4038776.

[11] N. Sydney, B. Smyth, and D. A. Paley, "Dynamic control of autonomous quadrotor flight in an estimated wind field," in *52nd IEEE Conference on Decision and Control*, IEEE, Dec. 2013, pp. 3609–3616. doi: 10.1109/CDC.2013.6760438.

[12] A. Zyluk and K. Sibilski, "The Gust Resistant MAV - Aerodynamic Measurements, Performance Analysis, and Flight Tests," in *AIAA Atmospheric Flight Mechanics Conference*, Reston, Virginia: American Institute of Aeronautics and Astronautics, Jan. 2015. doi: 10.2514/6.2015-1684.

[13] S. Park, W. Eun, and S. J. Shin, "Hybrid Analysis for Quadrotor Type UAV and Modified Blade Element Momentum Theory Considering Gust and Flight Condition," in *AIAA Scitech 2019 Forum*, Reston, Virginia: American Institute of Aeronautics and Astronautics, Jan. 2019. doi: 10.2514/6.2019-1329.

[14] F. Li, W.-P. Song, B.-F. Song, and J. Jiao, "Dynamic Simulation and Conceptual Layout Study on a Quad-Plane in VTOL Mode in Wind Disturbance Environment," *Int. J. Aerosp. Eng.*, vol. 2022, pp. 1–24, Jan. 2022, doi: 10.1155/2022/5867825.

[15] J. Paredes *et al.*, "Development, implementation, and experimental outdoor evaluation of quadcopter controllers for computationally limited embedded systems," *Annu. Rev. Control*, vol. 52, pp. 372–389, Jan. 2021, doi: 10.1016/j.arcontrol.2021.06.001.

[16] R. Fessi and S. Bouallègue, "LQG controller design for a quadrotor UAV based on particle swarm optimization," *Int. J. Autom. Control*, vol. 13, no. 5, p. 569, 2019, doi: 10.1504/IJAAC.2019.101910.

[17] İ. Şahin and C. Ulu, "Altitude control of a quadcopter using interval type-2 fuzzy controller with dynamic footprint of uncertainty," *ISA Trans.*, vol. 134, pp. 86–94, Mar. 2023, doi: 10.1016/j.isatra.2022.08.020.

[18] A. Fahruzi and A. Muharror, "Implementation Of Fuzzy Logic to Identify Accident Categories In SMS-Based Two-Wheeled Vehicles," *Inf. J. Ilm. Bid. Teknol. Inf. dan Komun.*, vol. 9, no. 1, pp. 89–94, Feb. 2024, doi: 10.25139/inform.v9i1.7555.

[19] Dodit Suprianto, Muhammad Taufik Prayitno, and Luqman Affandi, "Smart Greenhouse Coffee Dryer with Fuzzy Algorithm on Internet of Things Platform," *Inf. J. Ilm. Bid. Teknol. Inf. dan Komun.*, vol. 7, no. 1, pp. 1–8, Jan. 2022, doi: 10.25139/inform.v7i1.4163.

[20] Q. Liang and J. M. Mendel, "Interval type-2 fuzzy logic systems: Theory and design," *IEEE Trans. Fuzzy Syst.*, vol. 8, no. 5, pp. 535–550, 2000, doi: 10.1109/91.873577.

[21] Pavan N, "Design of Tiltrotor VTOL and Development of Simulink Environment for Flight Simulations," *Des. Tiltrotor VTOL Dev. Simulink Environ. Flight Simulations*, August, 2020.

[22] B. L. Stevens, F. L. Lewis, and E. N. Johnson, *Aircraft Control And Simulation Third Edition*, Third. 2015.

[23] A. Mathur and E. M. Atkins, "Design, modeling and hybrid control of a quadplane," *AIAA Scitech 2021 Forum*, January, pp. 1–16, 2021, doi: 10.2514/6.2021-0374.

[24] L. Zhou, J. Yang, T. Strampe, and U. Klingauf, "Incremental nonlinear dynamic inversion based path-following control for a hybrid quad-plane unmanned aerial vehicle," *Int. J. Robust Nonlinear Control*, vol. 33, no. 17, pp. 10304–10327, Nov. 2023, doi: 10.1002/rnc.6503.

[25] R. W. Beard and T. W. McLAIN, *Small unmanned aircraft*. Princeton University Press, 2012.

[26] L. Hanson, H. K. Jawahar, S. S. Vemuri, and M. Azarpeyvand, "Experimental investigation of propeller noise in ground effect," *J. Sound Vib.*, vol. 559, no. April, 2023, doi: 10.1016/j.jsv.2023.117751.

[27] F. Wahab, A. Sumardiono, A. R. Al Tahtawi, and A. F. A. Mulayari, "Desain dan Purwarupa Fuzzy Logic Control untuk Pengendalian Suhu Ruangan," *J. Teknol. Rekayasa*, vol. 2, no. 1, p. 1, 2017, doi: 10.31544/jtera.v2.i1.2017.1-8.

[28] K. Oguz Canbek and Y. Oniz, "Real-Time Implementation of an Interval Type-2 Fuzzy Logic Controller for the Trajectory Tracking of an UAV," *ISMSIT 2021 - 5th Int. Symp. Multidiscip. Stud. Innov. Technol. Proc.*, pp. 418–423, 2021, doi: 10.1109/ISMSIT52890.2021.9604539.

[29] L. A. Zadeh, "Fuzzy logic," *Computer (Long. Beach. Calif).*, vol. 21, no. 4, pp. 83–93, Apr. 1988, doi: 10.1109/2.53.

[30] L. A. Zedeh, "Knowledge representation in fuzzy logic," *IEEE Trans. Knowl. Data Eng.*, vol. 1, no. 1, pp. 89–100, Mar. 1989, doi: 10.1109/69.43406.

[31] Qilian Liang and J. M. Mendel, "Interval type-2 fuzzy logic systems: theory and design," *IEEE Trans. Fuzzy Syst.*, vol. 8, no. 5, pp. 535–550, 2000, doi: 10.1109/91.873577.

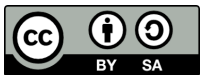

DOI : https://doi.org/10.25139/inform.v11i1.9644